



## Rapid microneedle fabrication by heating and photolithography

Himanshu Kathuria<sup>a</sup>, Kristacia Kang<sup>a</sup>, Junyu Cai<sup>b,c</sup>, Lifeng Kang<sup>c,\*</sup>

<sup>a</sup> Department of Pharmacy, National University of Singapore, Singapore 117543, Singapore

<sup>b</sup> China State Institute of Pharmaceutical Industry, Shanghai 201203, China

<sup>c</sup> School of Pharmacy, University of Sydney, Sydney, NSW 2006, Australia



### ARTICLE INFO

#### Keywords:

Dissolving microneedles  
PVP  
Thermal  
Photolithography  
Microneedle  
Fabrication

### ABSTRACT

Many fabrication methods for microneedle (MN) involve harsh conditions and long drying time. This study aims to fabricate a dissolving MN patch in a simple and efficient manner under mild conditions, using a combination of thermal and photo polymerisation. The MN patch was fabricated by pre-polymerisation of vinylpyrrolidone solution with heating followed by photolithography. The heating temperature and time of pre-polymer solution curing were optimized based on viscosity measurement. The MN properties including shape, size, skin penetration, dissolution, moisture absorption were determined. The fabricated MNs were sharp and consistent. The heated N-vinylpyrrolidone solution required less UV exposure time, thus reducing the total fabrication time. The percentage of MN penetration in human cadaver skin was more than 33.9%. The MN was dissolved within 1–2 min in water, or 40 min in saturated water vapor.

### 1. Introduction

Transdermal delivery is a useful way for drug administration, reducing the first-pass drug degradation and other side effects. Stratum corneum, the topmost layer of skin, while playing a significant role in protecting body from environmental noxious substances, impedes drug penetration through skin (Marwah et al., 2016). Hydrophilic drugs and large molecules show low permeability via passive diffusion. To this end, several techniques, such as chemical enhancement (Shen et al., 2018), iontophoresis (Chen et al., 2009), electroporation (Wei et al., 2014), acoustical methods (Alexiades, 2015), microneedles (MN) (Daugherty and Mrsny, 2003; Kathuria et al., 2015a; Kathuria et al., 2016; Kochhar et al., 2013b; Li et al., 2015; Prausnitz and Langer, 2008; Prausnitz et al., 2004), have been developed to enhance drug permeation through skin.

The application of MN is to pierce into the skin surface and create micron-sized passages, enabling the absorption of macromolecules into and/or through the skin (Gill et al., 2008; Liu et al., 2014). In the past few decades, several types of MN have been developed, including solid MN, coated MN, hollow MN and dissolving MN (Kim et al., 2012). Recently, Li et al reported solid effervescent MN patches to deliver contraceptives facilitating long-acting contraception (Li et al., 2019). The administration by dissolving MN made from biocompatible materials eliminates the risk of needle breakage in the skin and biohazardous

sharp waste. Dissolving MN patches have been reported to deliver proteins, nucleic acids and vaccines (Chen et al., 2015; Kathuria et al., 2015b; Kochhar et al., 2014; Kochhar et al., 2013a; Koh et al., 2018; Lee et al., 2015; Li et al., 2015; Song et al., 2012; Sun et al., 2015). Recently, an influenza vaccine delivered by dissolving MN patches completed a clinical trial (Rouphael et al., 2017).

To fabricate dissolving MN, several methods have been developed, including photolithography (Kochhar et al., 2014), drawing lithography (Fleischmann et al., 2012), droplet-born air blowing (Kim et al., 2013), and electro-drawing (Vecchione et al., 2014). The electro-drawing relies on surface drawing and quick solidifying, which is rapid but has less design flexibility than moulding. The drawing lithography has limited material selections and requires high temperature (Fleischmann et al., 2012). The droplet-born air blowing requires accurate control of machine function, e.g., uniform and intense air blowing for quick drying (Kim et al., 2013). The soft lithography method is fast and scalable but need high temperature (Moga et al., 2013). Moulding method is low-cost and operated in mild condition but needs long drying time (Lee et al., 2008; Vassilieva et al., 2015).

Sullivan, S. P et al reported the use of photo-polymerisation and micromoulding to fabricate dissolving MN with polyvinylpyrrolidone (PVP) (Sullivan et al., 2010; Sullivan et al., 2008). In liquid form at room temperature, the monomer of PVP, i.e., N-vinylpyrrolidone, can be polymerised by UV irradiation (Fig. 1). It avoids the addition of

\* Corresponding author at: School of Pharmacy, Faculty of Medicine and Health, Pharmacy and Bank Building A15, Science Road, University of Sydney, Sydney, NSW 2006, Australia.

E-mail address: [lifeng.kang@sydney.edu.au](mailto:lifeng.kang@sydney.edu.au) (L. Kang).

<https://doi.org/10.1016/j.ijpharm.2019.118992>

Received 8 October 2019; Received in revised form 7 December 2019; Accepted 22 December 2019

Available online 26 December 2019

0378-5173/ © 2019 Elsevier B.V. All rights reserved.

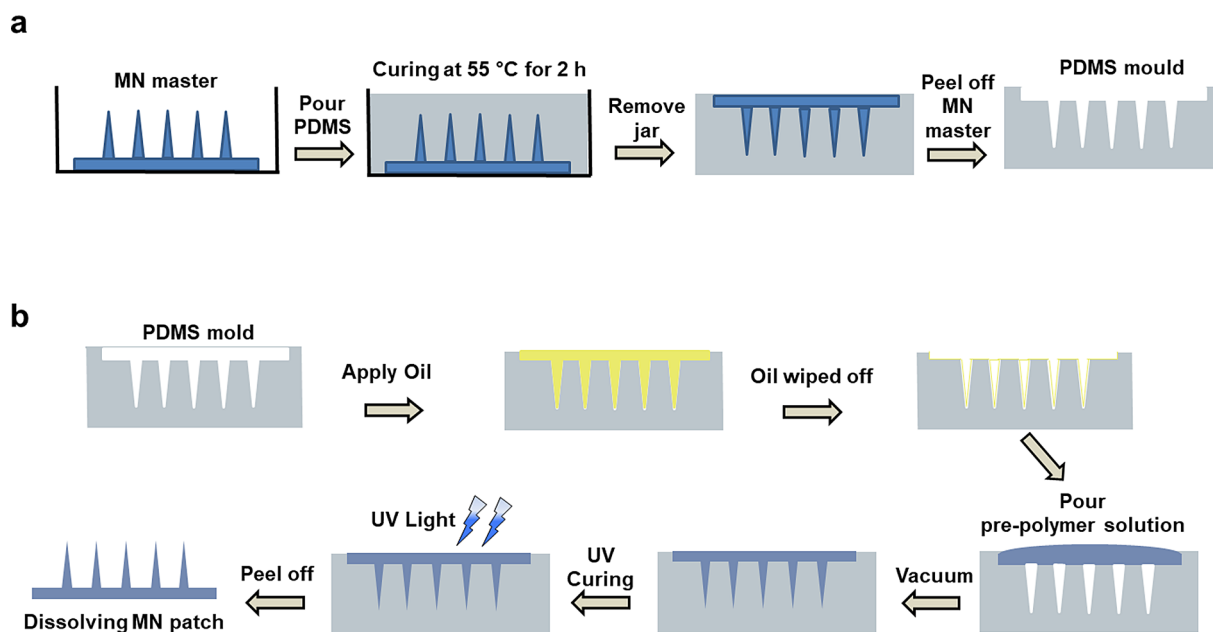


Fig. 1. Fabrication of micromould and dissolving MN patch. The schematic representation of fabrication process of mould (a) using MN master and dissolving MN (b) using PDMS mould.

organic solvent. With no subsequent drying process, the fabrication process is faster than other moulding methods. Nonetheless, this fabrication process requires more than 30 min of UV exposure, which may cause drug degradation and prolong the fabrication time.

To this end, we hypothesize that the UV exposure time can be shortened by heating the pre-polymer solution prior to photocuring. Furthermore, the bioactive can be loaded after cooling the pre-polymerised solution, prior to photopolymerization. To examine the effect of heating on polymerisation and solidification, we studied the polymerisation of N-vinylpyrrolidone at various temperatures and recorded the solution viscosity. The mechanical properties, dissolution and skin penetration of the resultant MN were also studied.

## 2. Materials and methods

### 2.1. Materials

Polydimethylsiloxane (PDMS) was obtained from Dow Corning Corporation, Midland, USA. The 3M Microchannel Skin System (MSS) made of plastic consisting of MN in rectangular array (13 by 27 array, or 351 needles) with needle height of about 700  $\mu\text{m}$  and a tip-to-tip needle spacing of 500  $\mu\text{m}$  was used as MN master structure. The 1-vinyl-2-pyrrolidone was obtained from Merck, Germany. Hyaluronic acid (HA) (8–15 kDa) from Making Cosmetics Inc., USA; 4,4'-azobis (4-cyanovaleric acid) (ABCV) from Sigma Aldrich, USA. Water was purified with Millipore Direct-Q system. The ultra-pure grade phosphate-buffered saline (PBS) was obtained from Vivantis, Malaysia.

### 2.2. Fabrication of micromould

The moulds were fabricated via thermal curing of PDMS with embedded 3M MSS as the master structure. The elastomer and curing agent (10:1) (Kathuria et al., 2015b; Pan et al., 2013), was mixed in disposable plastic cups using a plastic spatula, vacuumed at -95 kPa for 10–20 min to remove the entrapped air bubbles. Thereafter, the de-aerated mixture was poured slowly into the plastic petri dish (35 mm  $\times$  10 mm, Nunclon, Denmark), touching the sides to prevent air entrapment, it was vacuumed again as necessary. Later, it was kept for curing in hot air oven at 70  $^{\circ}\text{C}$  for 2 h. The cured PDMS with 3M MSS was gently taken out from the petri dish using a surgical blade. The 3M

MSS was gently peeled off from the cured PDMS to get the PDMS mould to prepare PVP MN (Fig. 1b).

### 2.3. Examination of heating effect

#### 2.3.1. Viscosity

Amber glass bottles were equilibrated on the hotplates for 2 min, maintained at various temperatures (40, 60, 80 and 90  $^{\circ}\text{C}$ ). 2 mL of N-vinylpyrrolidone (containing 1% or 0.5% w/v ABCV) was added to the equilibrated amber glass bottles on the hotplate. Three replicates of the N-vinylpyrrolidone were placed on the hotplates at each temperature. The samples were taken from each bottle at various time points until the solution becomes very viscous or solidified. All samples were immediately stored at 4  $^{\circ}\text{C}$  to prevent further polymerisation due to residual heat in mixture, until they were analysed for viscosity on the same day using a cone and plate viscometer (Sheen Instruments, UK). The viscometer was set at temperature 25  $^{\circ}\text{C}$ , speed 750 rpm, preheat time 15 s, run time 20 s.

#### 2.3.2. UV fabrication time after thermal prepolymerisation

Pre-polymerised solution of varying viscosities, obtained after heating of N-vinylpyrrolidone (containing 1% w/v ABCV) at various temperatures, was UV-polymerised in a PDMS mould and the time to form MN was recorded. The UV exposure was performed in intervals of 2.5 min until the solution was solidified. This was tested by checking the surface with the stainless-steel spatula, where hard backing was taken as the end point of MN patch formation. The spatula method was validated by using a force gauge (supplementary information, S11).

### 2.4. Fabrication of MN

2 mL of N-vinylpyrrolidone (containing 1% w/v ABCV) was initially pre-polymerised using heat (for 2 min at 90  $^{\circ}\text{C}$ ) and then allowed to cool down for 1 min at room temperature. Thereafter, the pre-polymerised mixture was pipetted onto an oiled PDMS micromould as described in earlier section, vacuumed at -95 kPa for 10–20 min to fill the micro cavities. Subsequently, the system was irradiated with the UV light at 100 W (9 cm away from UV source) for 8 min (Fig. 1c). The hyaluronic acid (HA) was incorporated as a model cosmetic ingredient (Choi et al., 2017), to study the effect on skin penetration and effect on

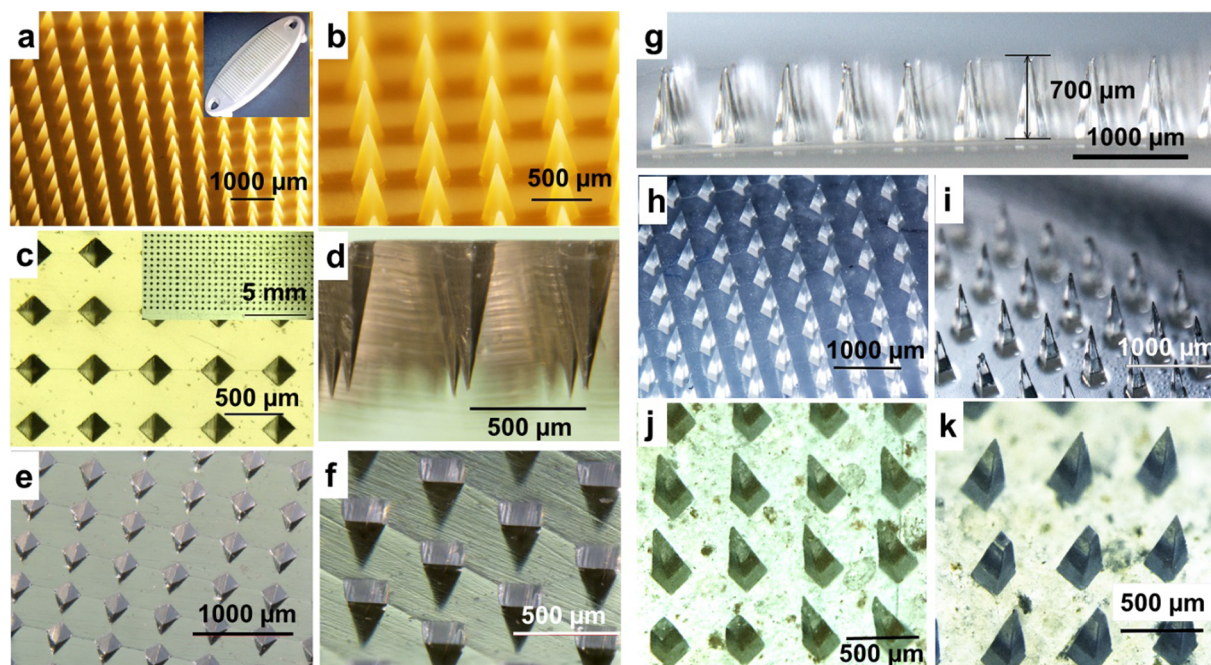


**Fig. 2.** Microscopic images of micromould and MN patches. (a-b) MN master. Microscopic top view (c), cross section (d) and side view (e-f) of fabricated PDMS mould. Microscopic image of blank PVP MN (g-i) and PVP MN with (j) 20% HA and (k) 40% HA.

moisture absorption. Shim et al, has also reported the combination of HA, PVP and carboxy methyl cellulose MN patch prepared using micromoulding drying (Shim et al., 2018). The super-low molecular weight HA (8–15 kDa) was added to PVP MN arrays at 20% and 40% w/v concentrations. The direct photolithography approach utilizing photomask was also studied to fabricate PVP MN.

### 2.5. Dissolution of MN

The dissolution of MN was tested in two conditions. First, a petridish was filled with 10 mL of distilled water and MN patch was individually submerged. In the second setup, a saturated moisture chamber was used. The MN patch was fixed on the glass slide using double-sided tape. The glass slide with MN patch was placed slanted in the cavity of self-designed PDMS structure kept in petridish. Before the addition of dissolution medium into the cavity, Nikon SMZ25 stereomicroscope (Nikon, Japan) was used to observe the MN array. Later, the cavity was filled with 20 mL of phosphate buffer saline to submerge the MN patch. The dissolution of MN patch was recorded under microscope. Similarly, the MN patch was also observed in saturated moisture condition.

### 2.6. MN penetration efficiency

The MN penetration efficiency was studied using an in vitro model (Larraneta et al., 2014; Quinn et al., 2015). Parafilm M® was folded into eight layers without stretching (~1 mm in thickness). The folded parafilm was placed on a cured PDMS support. The MN patch was placed onto the parafilm. Later, using a strain gauge (JSV H1000, JISC, Japan), the movable probe was lowered at 20 mm/min until a force of 25 N (0.06 M/needle) was exerted and held for 1 min. This load was chosen to mimic the average human thumb force (Mathiowetz et al., 1985). The paraffin film was then unfolded, and the number of penetrated holes in each layer was counted using a stereomicroscope.

Further investigation was done using human cadaver skin samples (Science Care, Phoenix, AZ, USA). The use of cadaver human skin for this study has been reviewed by the National University of Singapore Institutional Review Board and subsequently exempted because the cadaveric tissues used in this study were without identifiable private

information. The cadaver skin came from a 92-year-old Caucasian female. Frozen skin samples were thawed for 20 min at room temperature. Subsequently, it was cut into 4 cm × 4 cm pieces. The skin pieces were placed on wet tissue, and later kept aside for 15 min to equilibrate. The pressure was applied by using the strain gauge onto MN patch for it to penetrate the skin at 25 N for 1 min. The penetrated skin was flooded with trypan blue dye and left on skin for 30 min before rinsing away the excess dye with 70% ethanol, then wiped with tissue. The number of stained punctures was counted under stereomicroscope.

### 2.7. Skin histology

The human cadaver skin samples after penetration study were stored in 10% normal buffered formalin at 4 °C first, and later, soaked in 15% w/v sucrose solution overnight before cryo-sectioning. The samples were cross-sectioned using the a microcryostat (Leica, Germany) to obtain cross sections of 20 µm on gelatine-coated glass slide. The cross sections were stained according to standard protocols of haematoxylin and eosin (H&E) staining. The stained samples were imaged and analysed using the stereoscopic microscope.

## 3. Results

### 3.1. Characterisation of mould

The fabricated PDMS mould had satisfactory integrity and precision. The micro cavities with sharp tips were obtained. The micromould cavities were 13 × 27 array with a height of 700 µm and tip-to-tip distance of 500 µm (Fig. 2a-f).

### 3.2. Characterisation of MN

The MN formed by the new process was sharp and their dimensions followed the the master structure (Fig. 2g-k). The oiling step helped the removal of MN patch from the mould. The oiling was essential, without which the PDMS would be torn off from the micromould (SI2). The MN patch was hygroscopic, which tends to absorb moisture from the environment and softens in a few min. Therefore, the MN patches were

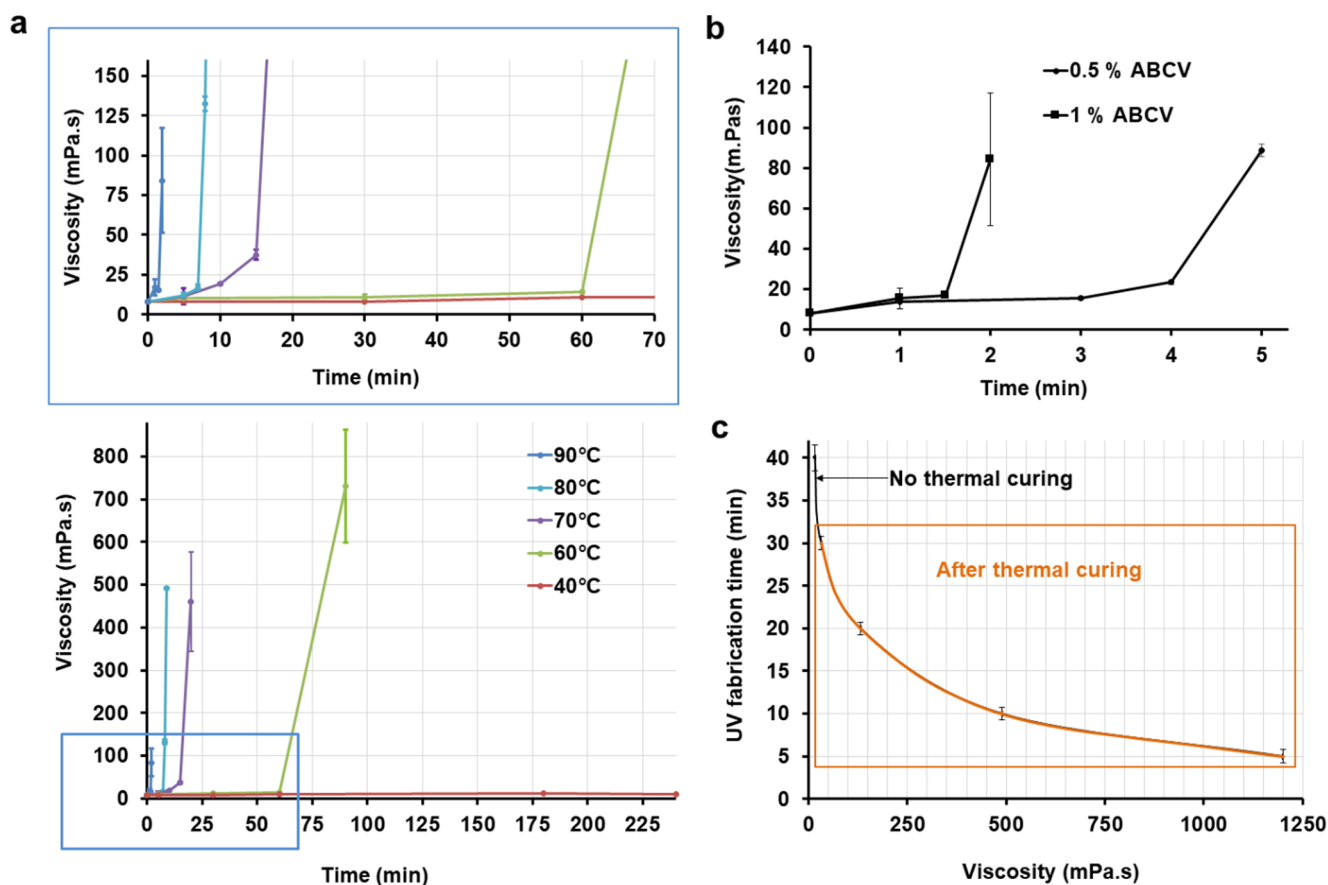


Fig. 3. Optimization of thermal polymerization. (a) Viscosity of VP solution (1% w/v ABCV) on heating at 40, 60, 70, 80 and 90 °C. (b) Effect of ABCV concentrations on viscosity on heating at 90 °C. (c) UV fabrication time of MN patch using varying viscosities of partially pre-polymerised mixture (thermal curing, 1% ABCV).

stored in a desiccator following fabrication. The fabrication involving direct photolithography and moulding with only thermal polymerization approach was unsuccessful (S13).

### 3.3. Effect of heating on fabrication

The ABCV serves as an initiator for both photo and thermal cross-linking. The heating effects on extent of polymerisation (expressed as viscosity) at different temperatures (40, 60, 80 and 90 °C) with varying time were investigated. It was observed that with increase in heating temperature of the pre-polymer solution, the polymerisation was faster (Fig. 3a). The amount of ABCV also affected the time of polymerisation. Compared to 0.5%, 1% w/v ABCV solution polymerised faster when heated at 90 °C (Fig. 3b). Moreover, the MN fabrication time (UV exposure time) decreases as viscosity of polymer solution increases (Fig. 3c). The increase in viscosity at a temperature with respect to time was a result of continuous thermal polymerisation. These form the basis of faster fabrication method for MN fabrication where N-vinylpyrrolidone was first thermo-polymerised followed by UV polymerisation in the mould. The UV polymerisation allowed the MN fabrication under mild condition at room temperature. Although the method of fabrication involved heating of N-vinylpyrrolidone monomer, active ingredients can be incorporated post-heating after the polymer solution has cooled down. The MN fabrication using thermal polymerisation and photolithography shortened the MN fabrication time, which can also potentially benefit the thermally unstable actives. The reduction in fabrication time was at least three times compared to direct UV polymerisation.

### 3.4. Dissolution of MN

The dissolution of MN occurred rapidly in water, which showed that it has the potential of rapidly delivering the bolus dose of active ingredients. Furthermore, when exposed to saturated moisture chamber, the MN were completely dissolved within 45 min (Fig. 4 and video).

### 3.5. MN penetration efficiency

The number of holes created by the array on each parafilm layer was counted to calculate the percentage penetration. Based from an earlier work (Larraneta et al., 2014), if penetration was counted as greater than 20% of all needles penetrated, the depth of insertion can be estimated from the thickness of the parafilm layers. The blank MN performed good penetration of 2 parafilm layers (Fig. 5a-b).

The penetration of the blank MN, 20% and 40% w/v HA MN were greater than 20% up to second layer. The thickness of parafilm layer was measured  $154 \pm 6.8 \mu\text{m}$ . The MN penetration depths of all MN patches were ranging 308–462  $\mu\text{m}$ . It was observed that percent penetration dropped as more HA (40 %w/v) was added to the MN (Fig. 5c). This may be due to the weak strength of the HA-loaded MN. It was also observed that 40% w/v HA MN patch has less number of fully formed MN. This could be attributed to interference in formation of the rigid MN structures or the MN being more brittle to break during removal from mould at higher HA concentration (40%, w/v). The MN also had good performance in the penetration of human skin (Fig. 6). The clear visible penetration in skin after trypan blue staining was > 33.9%. In addition, H&E stain also showed multiple penetration inside the treated skin. The depths of penetration of MN based on micropores were < 100  $\mu\text{m}$ . Furthermore, the MN tips were broken (Fig. 5b) after 1 min of application on human skin.

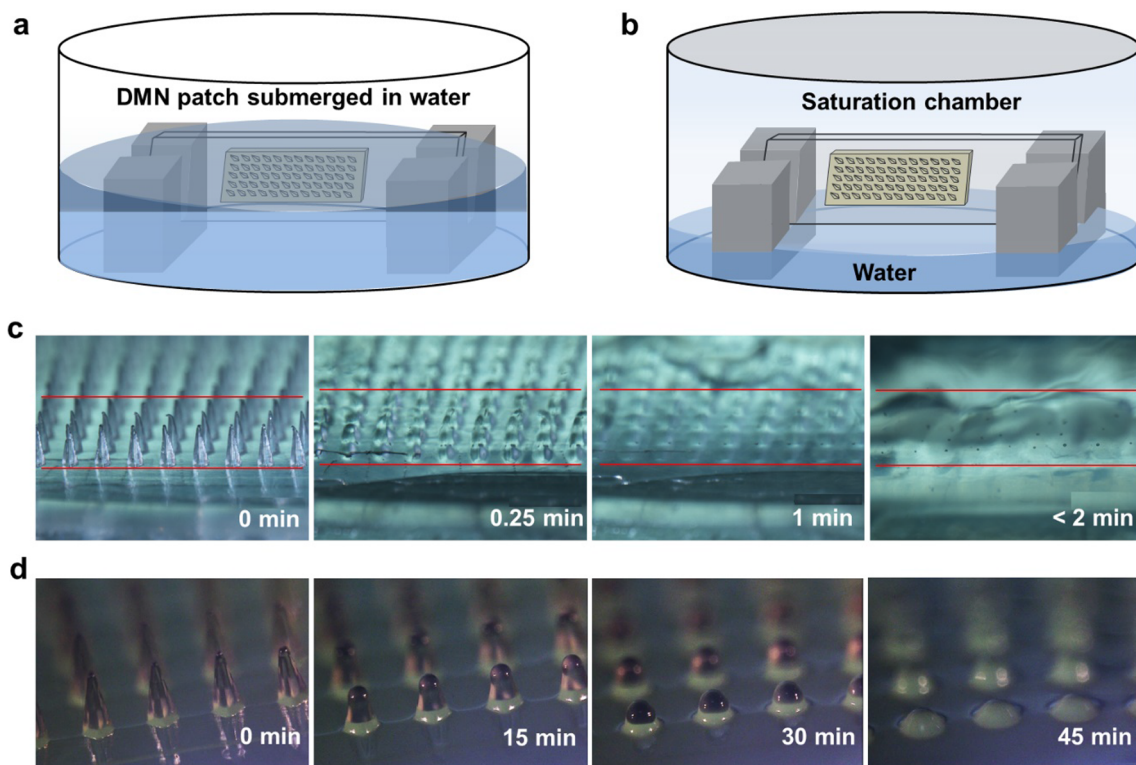


Fig. 4. In vitro dissolution of MN patch. (a) Schematic of dissolution setup for PVP MN patch submerged in the water. (b) Schematic of dissolution setup for PVP MN patch in saturated vapor in a sealed container. (c) Microscopic image of PVP MN showing dissolution in water. (d) Microscopic image of PVP MN showing dissolution in saturated vapor.

4. Discussion

We have fabricated dissolving MN patch utilizing thermal and photo-polymerisation. The resultant MN had similar geometry

resembling the master. Sullivan et al also used UV polymerisation to form PVP MN from N-vinylprolidone with 1.5% w/v azobisisobutyronitrile as the photoinitiator (Sullivan et al., 2008). In the present study, apart from UV polymerisation, we also utilized pre-

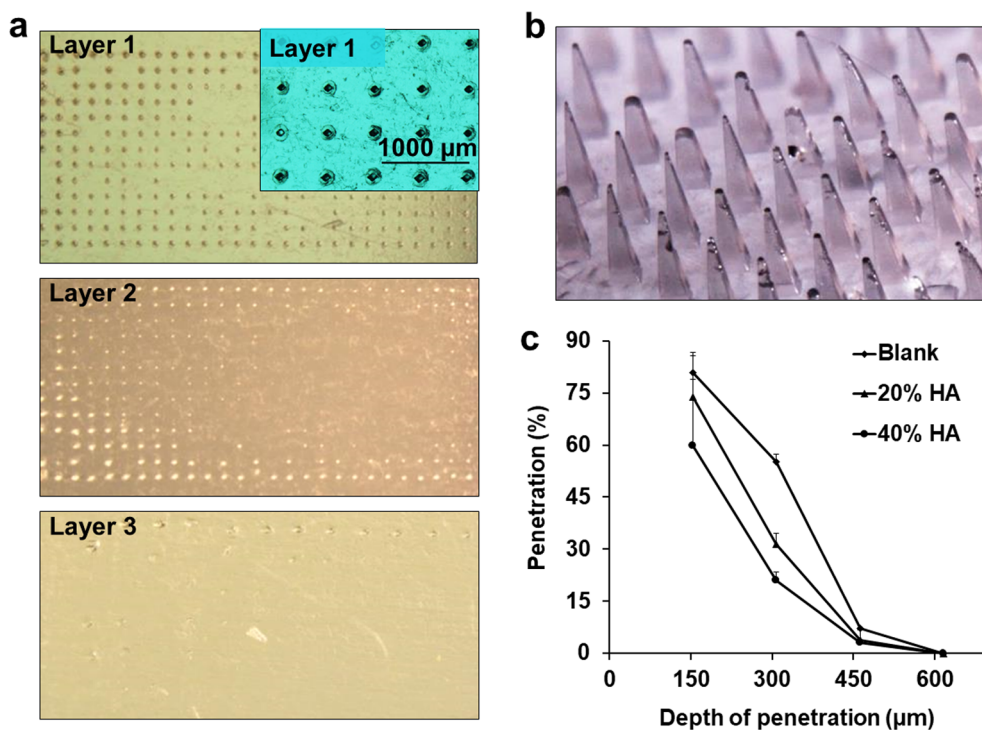
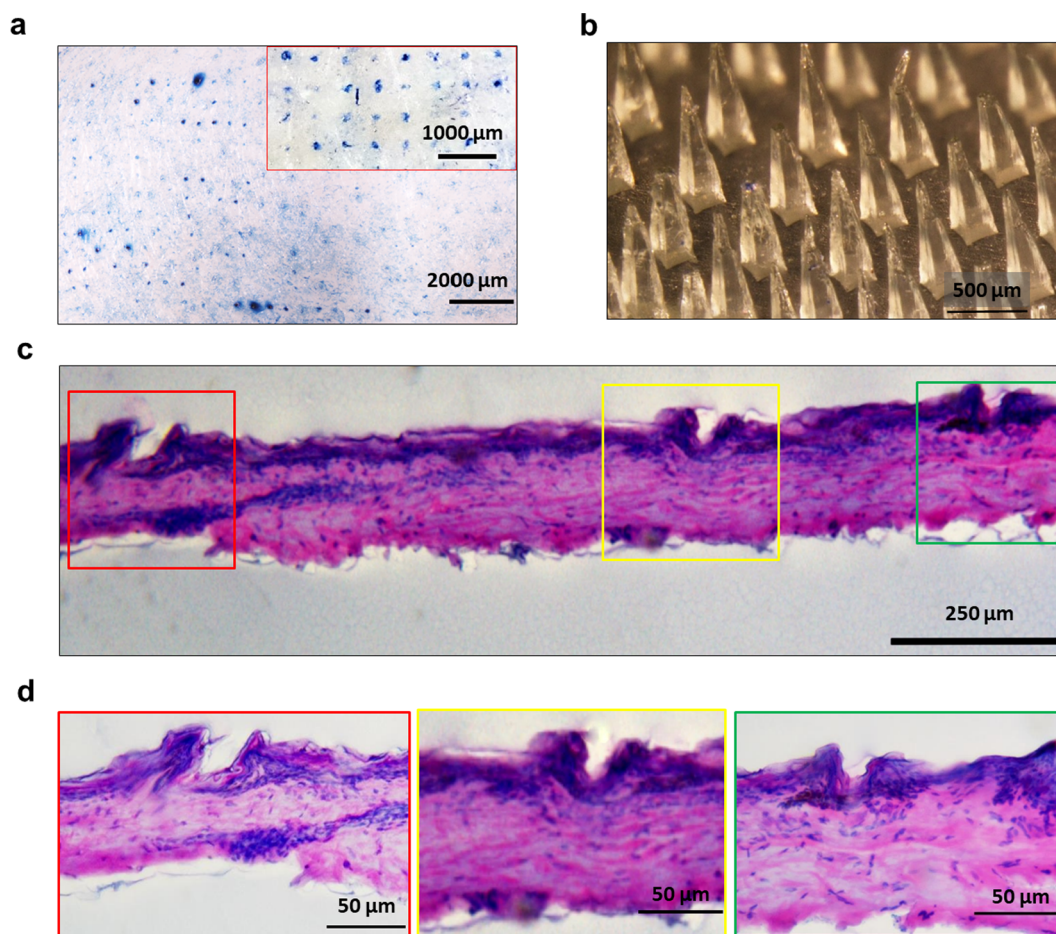


Fig. 5. MN patch penetration in parafilm layers. (a) Insertion of blank MN into parafilm layers 1–3. (b) MN after insertion into parafilm. (c) Percentage of insertion in each parafilm layer and insertion depths (calculated by considering the thickness of parafilm (154 ± 6.8 μm)).



**Fig. 6.** MN patch penetration in human cadaver skin. (a) Insertion of blank PVP MN into human cadaver skin stained with trypan blue. (b) MN after insertion into parafilm. (c-d) H & E stained images of MN treated skin showing micro-punctures. (For interpretation of the references to colour in this figure legend, the reader is referred to the web version of this article.)

polymerisation by thermal curing, which can accelerate the MN fabrication process. Moreover, the ABCV was used as bifunctional initiator (thermal and photo) at a concentration of less than 1% w/v.

Although the current fabrication added an additional heating step, it reduced the UV exposure time. The fabrication time may be reduced further for scale-up by optimisation of factors affecting thermal polymerisation, for e.g., heating time, heating temperature, bulk heating volume, mixing speed, etc. This will allow for the heating of N-vinylpyrrolidone solution in bulk; subsequently, large number of MN patch may be fabricated rapidly with reduced UV exposure time, which would increase fabrication turnover rate.

In addition, higher viscosity pre-polymer solution may be desirable if incorporated active ingredients need to be suspended in the pre-polymer solution. However, very high viscosity of pre-polymer mixture ( $> 1200$  mPa s) would need high vacuum for filling into micromould, thus selecting too high a viscosity may not be desirable. Nevertheless, for production of large numbers of MN patches, the current method may be more efficient.

The parafilm model has been widely used for skin penetration testing (Larraneta et al., 2014). However, the penetration efficiency of blank PVP MN into human cadaver skin was at least 33.9%, which was lower than the penetration efficiency of MN in parafilm model. This could be due to lower depth of penetration where all micropores were not stained by trypan blue and another reason could be wet surface of the cadaver skin, which causes rapid softening of MN.

The observation from moisture absorption also could support this attribute, which warrants the need of proper storage to avoid changes in mechanical strength (SI4). The thumb force (described as a force that

one would apply on elevator button) may range from about 10 to 40 N. The force of  $\sim 20$  N applied in this study has been estimated to be the medium force of the thumb for both male and female (Larraneta et al., 2014). As this study has demonstrated penetration with  $\sim 20$  N force with thumb, the MN patch would allow for comfortable insertion in self-administration by patients.

The dissolution of MN is a crucial information which is mostly studied using skin (Koh et al., 2018; Sullivan et al., 2008), gel (Nejad et al., 2018) and phosphate buffer. Here, the MN was partially intact (tips were broken) after 1 min of application onto human skin in the penetration study. This suggested that the dissolution of MN inside the skin cannot be as fast as dissolution in water.

Therefore, submerging the MN in water is not an ideal model of dissolution in human skin because the artificially high-water exposure would have been unrealistic and led to instant dissolution. In contrast, the dissolution testing in water vapor (Fig. 4) would be more suitable for dissolution study. This condition would be closer to skin condition where the MN after skin penetration will not come into immediate contact with the bulk fluid, rather it slowly swells, followed by dissolution in interstitial fluid inside skin.

In terms of toxicity, PVP has a long-standing reputation to be safe for human use, for instance, as an excipient for tableting. Moreover, Sullivan et al reported that PVP with molecular weight less than 25 kDa get excreted via urinary excretion (Sullivan et al., 2010; Sullivan et al., 2008). The fabricated PVP MN was estimated to have lower molecular weights (SI5). After insertion of MN into skin, PVP will dissolve in the interstitial fluids of skin, and then be eliminated via urine. Similarly, ABCV also showed acceptable safety profile. It had been used as the

initiator for N-vinylpyrrolidone copolymer ocular insert in an in vivo study with albino rabbits (Barbu et al., 2005). In another study, the cytotoxicity testing of photo-polymerized hydrogels containing ABCV for use as burn dressing was reported to be non-cytotoxic (Nalampang et al., 2013).

## 5. Conclusions

We fabricated dissolving MN with minimal UV exposure and accelerated fabrication process. The findings are potentially useful for upscaling MN patch mass production.

## Credit authorship contribution statement

**Himanshu Kathuria:** Writing - original draft, Visualization, Project administration, Investigation. **Kristacia Kang:** Writing - original draft, Visualization, Investigation. **Junyu Cai:** Writing - original draft, Visualization, Validation. **Lifeng Kang:** Funding acquisition, Supervision, Writing - review & editing, Conceptualization.

## Declaration of Competing Interest

The authors declare that they have no known competing financial interests or personal relationships that could have appeared to influence the work reported in this paper.

## Acknowledgements

We thank Teresa Ang for her kind assistance for the viscosity testing, and grant support from the National University of Singapore and the University of Sydney.

## Appendix A. Supplementary material

Supplementary data to this article can be found online at <https://doi.org/10.1016/j.ijpharm.2019.118992>.

## References

- Alexiades, M., 2015. Randomized, double-blind, split-face study evaluating fractional ablative erbium:YAG laser-mediated trans-epidermal delivery of cosmetic actives and a novel acoustic pressure wave ultrasound technology for the treatment of skin aging, melasma, and acne scars. *J. Drugs Dermatol.* 14, 1191–1198.
- Barbu, E., Sarvaiya, I., Green, K.L., Nevell, T.G., Tsibouklis, J., 2005. Vinylpyrrolidone-co-(meth)acrylic acid inserts for ocular drug delivery: synthesis and evaluation. *J. Biomed. Mater. Res. A* 74, 598–606. <https://doi.org/10.1002/jbm.a.30329>.
- Chen, H., Zhu, H., Zheng, J., Mou, D., Wan, J., Zhang, J., Shi, T., Zhao, Y., Xu, H., Yang, X., 2009. Iontophoresis-driven penetration of nanovesicles through microneedle-induced skin microchannels for enhancing transdermal delivery of insulin. *J. Control Release*. 139, 63–72. <https://doi.org/10.1016/j.jconrel.2009.05.031>.
- Chen, M.C., Ling, M.H., Kusuma, S.J., 2015. Poly-gamma-glutamic acid microneedles with a supporting structure design as a potential tool for transdermal delivery of insulin. *Acta Biomater.* 24, 106–116. <https://doi.org/10.1016/j.actbio.2015.06.021>.
- Choi, S.Y., Kwon, H.J., Ahn, G.R., Ko, E.J., Yoo, K.H., Kim, B.J., Lee, C., Kim, D., 2017. Hyaluronic acid microneedle patch for the improvement of crow's feet wrinkles. *Dermatol. Ther.* 30. <https://doi.org/10.1111/dth.12546>.
- Daugherty, A.L., Mrsny, R.J., 2003. Emerging technologies that overcome biological barriers for therapeutic protein delivery. *Expert. Opin. Biol. Ther.* 3, 1071–1081. <https://doi.org/10.1517/14712598.3.7.1071>.
- Fleischmann, R., Cutolo, M., Genovese, M.C., Lee, E.B., Kanik, K.S., Sadis, S., Connell, C.A., Gruben, D., Krishnaswami, S., Wallenstein, G., Wilkinson, B.E., Zwillich, S.H., 2012. Phase IIb dose-ranging study of the oral JAK inhibitor tofacitinib (CP-690,550) or adalimumab monotherapy versus placebo in patients with active rheumatoid arthritis with an inadequate response to disease-modifying antirheumatic drugs. *Arthritis Rheum.* 64, 617–629. <https://doi.org/10.1002/art.33383>.
- Gill, H.S., Denson, D.D., Burris, B.A., Prausnitz, M.R., 2008. Effect of microneedle design on pain in human volunteers. *Clin. J. Pain.* 24, 585–594. <https://doi.org/10.1097/AJP.0b013e31816778f9>.
- Kathuria, H., Fong, M.H., Kang, L., 2015a. Fabrication of photomasks consisting microlenses for the production of polymeric microneedle array. *Drug Deliv. Transl. Res.* 5, 438–450. <https://doi.org/10.1007/s13346-015-0245-z>.
- Kathuria, H., Kochhar, J.S., Fong, M.H., Hashimoto, M., Iliescu, C., Yu, H., Kang, L., 2015b. Polymeric Microneedle Array Fabrication by Photolithography. *J. Vis. Exp.* 105, e52914. <https://doi.org/10.3791/52914>.

- Kathuria, H., Li, H., Pan, J., Lim, S.H., Kochhar, J.S., Wu, C., Kang, L., 2016. Large size microneedle patch to deliver lidocaine through skin. *Pharm. Res.* 33, 2653–2667. <https://doi.org/10.1007/s11095-016-1991-4>.
- Kim, J.D., Kim, M., Yang, H., Lee, K., Jung, H., 2013. Droplet-born air blowing: novel dissolving microneedle fabrication. *J. Control Release*. 170, 430–436. <https://doi.org/10.1016/j.jconrel.2013.05.026>.
- Kim, Y.C., Park, J.H., Prausnitz, M.R., 2012. Microneedles for drug and vaccine delivery. *Adv. Drug Deliv. Rev.* 64, 1547–1568. <https://doi.org/10.1016/j.addr.2012.04.005>.
- Kochhar, J.S., Anbalagan, P., Shelar, S.B., Neo, J.K., Iliescu, C., Kang, L., 2014. Direct microneedle array fabrication off a photomask to deliver collagen through skin. *Pharm. Res.* 31, 1724–1734. <https://doi.org/10.1007/s11095-013-1275-1>.
- Kochhar, J.S., Lim, W.X., Zou, S., Foo, W.Y., Pan, J., Kang, L., 2013a. Microneedle integrated transdermal patch for fast onset and sustained delivery of lidocaine. *Mol. Pharm.* 10, 4272–4280. <https://doi.org/10.1021/mp400359w>.
- Kochhar, J.S., Quek, T.C., Soon, W.J., Choi, J., Zou, S., Kang, L., 2013b. Effect of microneedle geometry and supporting substrate on microneedle array penetration into skin. *J. Pharm. Sci.* 102, 4100–4108. <https://doi.org/10.1002/jps.23724>.
- Koh, K.J., Liu, Y., Lim, S.H., Loh, X.J., Kang, L., Lim, C.Y., Phua, K.K.L., 2018. Formulation, characterization and evaluation of mRNA-loaded dissolvable polymeric microneedles (RNApatch). *Sci. Rep.* 8, 11842. <https://doi.org/10.1038/s41598-018-30290-3>.
- Larraneta, E., Moore, J., Vicente-Perez, E.M., Gonzalez-Vazquez, P., Lutton, R., Woolfson, A.D., Donnelly, R.F., 2014. A proposed model membrane and test method for microneedle insertion studies. *Int. J. Pharm.* 472, 65–73. <https://doi.org/10.1016/j.ijpharm.2014.05.042>.
- Lee, I.C., He, J.-S., Tsai, M.-T., Lin, K.-C., 2015. Fabrication of a novel partially dissolving polymer microneedle patch for transdermal drug delivery. *J. Mater. Chem. B* 3, 276–285. <https://doi.org/10.1039/c4tb01555j>.
- Lee, J.W., Park, J.H., Prausnitz, M.R., 2008. Dissolving microneedles for transdermal drug delivery. *Biomaterials* 29, 2113–2124. <https://doi.org/10.1016/j.biomaterials.2007.12.048>.
- Li, H., Low, Y.S., Chong, H.P., Zin, M.T., Lee, C.Y., Li, B., Leolukman, M., Kang, L., 2015. Microneedle-mediated delivery of copper peptide through skin. *Pharm. Res.* 32, 2678–2689. <https://doi.org/10.1007/s11095-015-1652-z>.
- Li, W., Tang, J., Terry, R.N., Li, S., Brunie, A., Callahan, R.L., Noel, R.K., Rodriguez, C.A., Schwendeman, S.P., Prausnitz, M.R., 2019. Long-acting reversible contraception by effervescent microneedle patch. *Sci. Adv.* 5, eaaw8145. <https://doi.org/10.1126/sciadv.aaw8145>.
- Liu, S., Jin, M.N., Quan, Y.S., Kamiyama, F., Kusamori, K., Katsumi, H., Sakane, T., Yamamoto, A., 2014. Transdermal delivery of relatively high molecular weight drugs using novel self-dissolving microneedle arrays fabricated from hyaluronic acid and their characteristics and safety after application to the skin. *Eur. J. Pharm. Biopharm.* 86, 267–276. <https://doi.org/10.1016/j.ejpb.2013.10.001>.
- Marwah, H., Garg, T., Goyal, A.K., Rath, G., 2016. Permeation enhancer strategies in transdermal drug delivery. *Drug Deliv.* 23, 564–578. <https://doi.org/10.3109/10717544.2014.935532>.
- Mathiowetz, V., Kashman, N., Volland, G., Weber, K., Dowe, M., Rogers, S., 1985. Grip and pinch strength: normative data for adults. *Arch. Phys. Med. Rehabil.* 66, 69–74.
- Moga, K.A., Bickford, L.R., Geil, R.D., Dunn, S.S., Pandya, A.A., Wang, Y., Fain, J.H., Archuleta, C.F., O'Neill, A.T., Desimone, J.M., 2013. Rapidly-dissolvable microneedle patches via a highly scalable and reproducible soft lithography approach. *Adv. Mater.* 25, 5060–5066. <https://doi.org/10.1002/adma.201300526>.
- Nalampang, K., Panjakha, R., Molloy, R., Tighe, B.J., 2013. Structural effects in photo-polymerized sodium AMPS hydrogels crosslinked with poly(ethylene glycol) diacrylate for use as burn dressings. *J. Biomater. Sci. Polym. Ed.* 24, 1291–1304. <https://doi.org/10.1080/09205063.2012.755601>.
- Nejad, H.R., Sadeqi, A., Kiaee, G., Sonkusale, S., 2018. Low-cost and cleanroom-free fabrication of microneedles. *Microsyst. Nanoeng.* 4. <https://doi.org/10.1038/micronano.2017.73>.
- Pan, J., Yung Chan, S., Common, J.E., Amini, S., Miserez, A., Birgitte Lane, E., Kang, L., 2013. Fabrication of a 3D hair follicle-like hydrogel by soft lithography. *J. Biomed. Mater. Res. A* 101, 3159–3169. <https://doi.org/10.1002/jbm.a.34628>.
- Prausnitz, M.R., Langer, R., 2008. Transdermal drug delivery. *Nat. Biotechnol.* 26, 1261–1268. <https://doi.org/10.1038/nbt.1504>.
- Prausnitz, M.R., Mitragotri, S., Langer, R., 2004. Current status and future potential of transdermal drug delivery. *Nat. Rev. Drug Discov.* 3, 115–124. <https://doi.org/10.1038/nrd1304>.
- Quinn, H.L., Bonham, L., Hughes, C.M., Donnelly, R.F., 2015. Design of a dissolving microneedle platform for transdermal delivery of a fixed-dose combination of cardiovascular drugs. *J. Pharm. Sci.* 104, 3490–3500. <https://doi.org/10.1002/jps.24563>.
- Rouphael, N.G., Paine, M., Mosley, R., Henry, S., McAllister, D.V., Kalluri, H., Pewin, W., Frew, P.M., Yu, T., Thornburg, N.J., Kabbani, S., Lai, L., Vassilieva, E.V., Skountzou, I., Compans, R.W., Mulligan, M.J., Prausnitz, M.R., Beck, A., Edepuganti, S., Heeke, S., Kelley, C., Nesheim, W., 2017. The safety, immunogenicity, and acceptability of inactivated influenza vaccine delivered by microneedle patch (TIV-MNP 2015): a randomised, partly blinded, placebo-controlled, phase 1 trial. *The Lancet* 390, 649–658. [https://doi.org/10.1016/s0140-6736\(17\)30575-5](https://doi.org/10.1016/s0140-6736(17)30575-5).
- Shen, M., Liu, C., Wan, X., Farah, N., Fang, L., 2018. Development of a daphnetin transdermal patch using chemical enhancer strategy: insights of the enhancement effect of Transcutol P and the assessment of pharmacodynamics. *Drug Dev. Ind. Pharm.* 44, 1642–1649. <https://doi.org/10.1080/03639045.2018.1483391>.
- Shim, W.S., Hwang, Y.M., Park, S.G., Lee, C.K., Kang, N.G., 2018. Role of polyvinylpyrrolidone in dissolving microneedle for efficient transdermal drug delivery: in vitro and clinical studies. *Bull. Korean Chem. Soc.* 39, 789–793. <https://doi.org/10.1002/bkcs.11476>.

- Song, J.M., Kim, Y.C., Eunju, O., Compans, R.W., Prausnitz, M.R., Kang, S.M., 2012. DNA vaccination in the skin using microneedles improves protection against influenza. *Mol. Ther.* 20, 1472–1480. <https://doi.org/10.1038/mt.2012.69>.
- Sullivan, S.P., Koutsonanos, D.G., Del Pilar Martin, M., Lee, J.W., Zarnitsyn, V., Choi, S.O., Murthy, N., Compans, R.W., Skountzou, I., Prausnitz, M.R., 2010. Dissolving polymer microneedle patches for influenza vaccination. *Nat. Med.* 16, 915–920. <https://doi.org/10.1038/nm.2182>.
- Sullivan, S.P., Murthy, N., Prausnitz, M.R., 2008. Minimally invasive protein delivery with rapidly dissolving polymer microneedles. *Adv. Mater.* 20, 933–938. <https://doi.org/10.1002/adma.200701205>.
- Sun, W., Inayathullah, M., Manoukian, M.A., Malkovskiy, A.V., Manickam, S., Marinkovich, M.P., Lane, A.T., Tayebi, L., Seifalian, A.M., Rajadas, J., 2015. Transdermal delivery of functional collagen via polyvinylpyrrolidone microneedles. *Ann. Biomed. Eng.* 43, 2978–2990. <https://doi.org/10.1007/s10439-015-1353-0>.
- Vassilieva, E.V., Kalluri, H., McAllister, D., Taherbhai, M.T., Esser, E.S., Pewin, W.P., Pulit-Penaloza, J.A., Prausnitz, M.R., Compans, R.W., Skountzou, I., 2015. Improved immunogenicity of individual influenza vaccine components delivered with a novel dissolving microneedle patch stable at room temperature. *Drug Deliv. Transl. Res.* 5, 360–371. <https://doi.org/10.1007/s13346-015-0228-0>.
- Vecchione, R., Coppola, S., Esposito, E., Casale, C., Vespini, V., Grilli, S., Ferraro, P., Netti, P.A., 2014. Electro-drawn drug-loaded biodegradable polymer microneedles as a viable route to hypodermic injection. *Adv. Funct. Mater.* 24, 3515–3523. <https://doi.org/10.1002/adfm.201303679>.
- Wei, Z., Zheng, S., Wang, R., Bu, X., Ma, H., Wu, Y., Zhu, L., Hu, Z., Liang, Z., Li, Z., 2014. A flexible microneedle array as low-voltage electroporation electrodes for in vivo DNA and siRNA delivery. *Lab Chip.* 14, 4093–4102. <https://doi.org/10.1039/c4lc00800f>.